Averting Extinction in Autothermal Catalytic Reactor Operations

A multiloop control system and an on-line reactor operability analysis were developed for the purpose of detecting and averting extinction of the autothermal state of a laboratory catalytic reactor. The reactor system consisted of a feed-effluent heat exchanger and two packed beds in which the exothermic reaction between hydrogen and oxygen occurred.

The strategy of control was based on the preservation of the relative stability of the autothermal steady state when the reactor experienced large changes in feed concentration and flow rate. Such a strategy involved a model-based prediction of reactor conditions that so preserved stability, and a procedure to guide the process rapidly and smoothly to those new conditions. Experiments demonstrated the successful avoidance of extinction and the orderly attainment of new operating conditions in about three reactor-system time constants. The procedures developed could serve as a component of an on-line expert system for safe reactor operations.

S. G. Metchis and A. S. Foss
Department of Chemical Engineering
University of California
Berkeley, CA 94720

Introduction

The autothermal state of a reactor system can die out or extinguish when there is a sustained drop in reactant feed concentration. The development of means to maintain reactor operability under such abnormal operating conditions is the objective of this work. An on-line reactor analysis and control system was developed that first detects imminent extinction and next guides the reactor to a new, safe operating condition. Such a system was developed with the dual objectives of retaining an acceptable degree of relative stability of the reactor and maintaining rangeability of the manipulatable inputs. The workability of the system was demonstrated on a laboratory reactor consisting the two catalyst beds in series in which hydrogen and oxygen reacted, a feed-effluent heat exchanger, and a feed preheat system.

The development of a strategy to avert loss of operability under abnormal conditions and the means of its execution in a timely manner has always been a concern of engineers in process operations, but such strategies for operating reactors have received little attention in the literature. One sobering account of the consequences of making incorrect operating decisions while attempting to correct for abnormal reactor conditions was given by Gerdes et al. (1977). The literature is replete, however, with analyses for reactor design, the best known of which are those of van Heerden (1953, 1958). Studies of the stability of autothermal reactors (Orcutt and Lamb, 1960; Baddour et al., 1965; Luss and Amundson, 1967) have given insight into the operations problems but have not provided strategies for correcting abnormal conditions. Modal and self-tuning control methods for stabilizing an unstable autothermal reactor system have been developed by Bonvin et al. (1983), Wong et al. (1983), and McDermott and Mellichamp (1983). Recent work by McDermott et al. (1984) has investigated multiloop self-tuning for both stable and unstable autothermal states. Stephens and Richards (1973) concentrated on the control of an ammonia synthesis reactor at stable operating points using a control criterion related to system stability. Like the work of Stevens and Richards, our work focuses on stable reactor systems but takes the further step of guiding the system from one stable operating point to another under abnormal operating conditions.

Our system is structured to first detect imminent extinction through a conventional steady-state energy balance analysis. This is done on-line. Next a determination is made (also on-line) of set points that would insure the retention of the autothermal

Correspondence concerning this paper should be addressed to A. S. Foss.
The present address of S. G. Metchis is Shell Development Co., Westhollow Research Center, Houston, TX.

condition (albeit a different condition), that would maintain the same degree of stability at the new condition, and that would position the most important manipulatable input at mid range after the new state had been reached. The combined analysis and search takes about 6 min on our 1975-vintage computer (modern machines would be at least ten times faster). These pieces of information are used to drive the set points of a multiloop network of conventional PI controllers that may be switched in and out of operation at various stages of the recovery. One of the control loops drives the temperature of the reactant stream entering the first catalyst bed to the new set point. Another drives a flow control loop to mid range. The system performs smoothly and robustly, being able to accommodate feed concentration dips that would have extinguished the autothermal state. The system also ably handles concentration increases, repeated changes in concentration, and large changes in feed rate.

One of the most important contributions of this work is the development of an on-line procedure to maintain operability through knowledge of model-derived set points. The set points so determined reflect the current state of the process. Relative stability is one of the criteria used for their selection; that seems to be new and of value in making reliable adjustments when abnormal conditions are encountered. Further, a key feature of the system is its modularity and use of well-established elements, namely steady-state reactor and heat exchanger models, conventional PI controllers, and a van Heerden analysis of the reactor steady state.

Reactor System and the Extinction Problem

The continuity of operation of autothermal reactor systems hinges on sustaining "ignition" of the reaction by raising the feed temperature high enough though heat exchange with the hot effluent gas. In the reactor system under discussion here, feed preheating under normal conditions is accomplished in a feed-effluent heat exchanger external to the reactor. Figure 1 shows the location of this feed-effluent exchanger directly above the reactor catalyst beds. Normally about 60% of the main feed is passed through the feed-effluent exchanger, the rest being evenly split between the bypass and quench streams shown in the figure. A local temperature controller attempts to regulate the temperature of the feed to bed I by calling for more or less bypass around this exchanger. The function of the other temperature control loops is described later. Such a reactor configuration and allocation of flows is typical of many found in industrial practice. The auxiliary heating system located above the reactor-exchanger simulates heat exchanger trains usually found upstream of industrial reactors and can be used in averting extinction of the reactor under abnormal conditions.

Extinction of this reactor-exchanger system occurs when process disturbances, such as a sustained decrease in feed oxygen

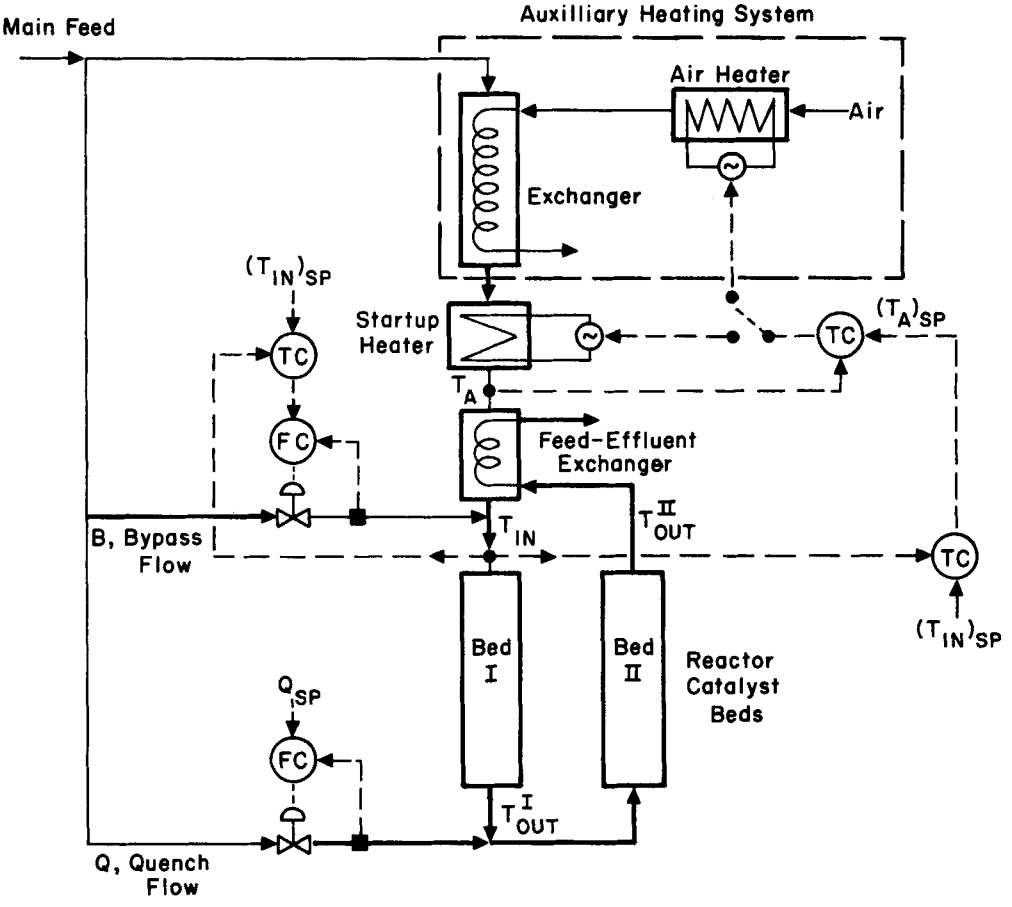

Figure 1. Autothermal reactor system and basic control loops.

concentration, deny the closure of the steady-state energy balance of the process. Conditions necessary for the existence of an autothermal steady state may be appreciated most easily through examination of a graph relating inlet and outlet temperatures of the reactor and exchanger, each as separate processes. Such a graph is shown in Figure 2 for conditions typical of those studied experimentally. The sigmoidal reactor curves are derived from steady-state differential material and energy balances applied to the one-dimensional, plug-flow reactor model described shortly. Curves for two feed concentrations are shown. The sharp rise in the reactor curve obtains from an exponential dependence of the reaction rate on temperature. The slight dip at high temperatures results from heat loss from the beds of the experimental reactor used; large industrial reactors would simply exhibit a knee here. The straight heat exchanger curves derive from energy balances on the two streams in the exchanger. The slope of these exchanger curves increases with bypass flow rate, and the intercept is determined by the temperature of the cold feed gas entering the exchanger. Steady states of the reactor-exchanger combination correspond to intersections of the two classes of curves, as is well known (van Heerden, 1953, 1958). Multiple intersections can occur (intersections *a*, *b*, and *c* in Figure 2) and did indeed occur under the conditions of this work. The steady state of interest here is the high-temperature state (intersection *c*). The precise location of this state is influenced in industrial circumstances by the economics of the particular processes and is reported (Baddour et al., 1965) in some instances to be near the blow-off point (intersection *d*). Thus, the range of bypass flow rate manipulation is bounded by blow-off and full valve closure (no bypass flow). The low conversion state (intersection *a*) and the unstable state (intersection *b*) are of little industrial interest. Extinction occurs when a high-temperature intersection disappears, as it does in the example of this diagram when the feed concentration drops from y_{F1} to y_{F2}. Movement of the exchanger curves by reduction of the bypass flow, in an attempt to retain an intersection, is seen to be thwarted by the encounter with a fully closed bypass valve. In a subsequent section, it is shown how the high-temperature steady state (and the autothermal condition) can be retained by a downward shift in the heat exchanger curve, accomplished by heating the feed stream by use of the auxiliary heating system shown in Figure 1.

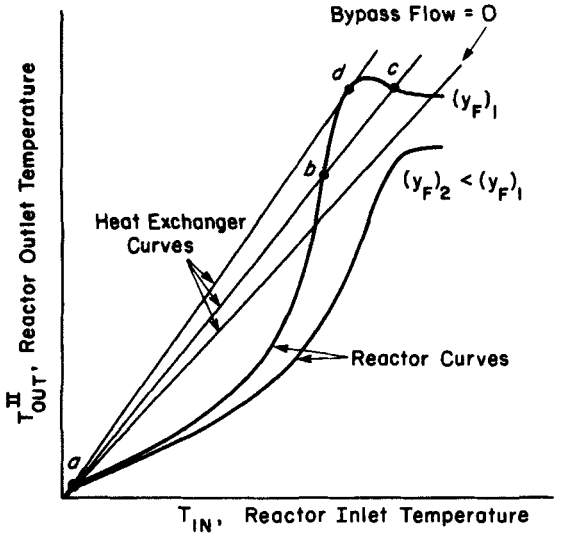

Figure 2. Steady-state relationships between the reactor inlet and outlet temperatures for reactor and heat exchanger.

Laboratory reactor system

The important dimensions of the reactor system components are given in Table 1. The two reactors and the feed-effluent exchanger are made entirely of glass and are constructed as separate modules that can be easily assembled and disassembled. The module in which the feed-effluent exchanger resides also contains the startup heater and the auxiliary exchanger. Heat loss from these three modules is minimized through use of silvered vacuum jackets, but nonetheless about one-quarter of the heat liberated by reaction is lost to the surroundings. Heat loss from the joints between modules is minimized through use of individual external heating tapes adjusted to equalize temperatures inside and outside the particular joint.

The coil of the feed-effluent exchanger was constructed with a tap-off port halfway along the coil so that the effluent gas could be passed through either the full coil or just the bottom half. Only half the coil was used in this work, a condition that resulted in an exchanger with about one heat-transfer unit on the shell side. Such a design accomplishes the heat exchange required for autothermal operation and also allows the auxiliary exchanger to participate in influencing the temperature at the top of bed I.

The auxiliary heating system was not operational at the time of these experiments (1981). Instead, the electric startup heater was used when called for by the control system. In later experi-

Table 1. Dimensions of Reactor System Components

Reactor Beds (all-glass construction)
Diameter: 2.60 cm ID, 2.84 cm OD
Length: 24.5 cm
Catalyst depth: 16.5 cm (bed I), 22.0 cm (bed II)
Catalyst: 0.5 mm silica gel particles, 0.015 wt. % platinum
Insulation: 5.5 cm ID silvered vacuum glass jacket
Feed-Effluent Exchanger (all-glass construction)
Shell diameter: 2.60 cm ID, 2.84 cm OD
Coil tubing: 3 mm ID, 5 mm OD, 31.5 cm long
Coil helix: 6 turns, 1.64 cm OD, 6 cm rise
Coil surface area: 29.7 cm^2 inside tube area
Insulation: same as reactor beds
Startup Heater
Shell diameter: same shell as feed-effluent exchanger
Heating element: 128 cm, 30 gauge nichrome wire
Element support: glass cage supported from top of shell
Auxiliary Heat Exchanger
Shell diameter: same shell as feed-effluent exchanger
Coil tubing: stainless steel, 0.318 cm OD, 85.8 cm long
Coil helix: 1.64 cm OD, 16 cm rise
Coil surface area: 63.8 cm^2
Insulation: same as reactor beds
Air Heater
Tube: stainless steel, 1.27 cm OD, 20 cm long
Heating element: nichrome wire, 400 W max power
Insulation: magnesia sleeve

ments (Lappinga and Foss, 1984) the full auxiliary heating system was used and coordinated with the system to avert extinction.

Provisions were made at several points in the apparatus for measurement of stream temperatures by bare thermocouples introduced through ports directly into the streams; such ports were provided every 5.5 cm along the length of the catalyst beds. Ports served also for continuously extracting small streams of gas for measurement of oxygen concentration. Gas concentration was measured with a paramagnetic oxygen analyzer.

Two temperature control loops are shown in Figure 1 (broken lines) for the purpose of identifying the set points $(T_{in})_{SP}$ and $(T_A)_{SP}$ as the major command inputs associated with our procedures for averting extinction. These loops, and others to be described later, are implemented by direct digital control algorithms in a minicomputer.

A typical profile of temperature in the system under steady autothermal conditions is shown in Figure 3. Here, predictions of a reactor model (presented later) are compared with measurements. Other properties and conditions of a typical autothermal state are given in Table 2. An important characteristic of the reactors recorded there is a 6 min thermal wave transit time in each catalyst bed. That compares with a 0.25 s gas residence time.

Measurements collected by the control computer, one of two in the computer system, consisted of temperatures at every port; flow rates of feed H_2, feed O_2, bypass, and quench streams; and one concentration, which could have been taken from any sample port but was usually taken from the bed II inlet. The feed concentration was inferred from the measured hydrogen and oxygen flows. The measurements were filtered and amplified, then multiplexed through a single analog/digital converter. The filter time constants were about 0.5 s for all measurements. A scan of all measurements was made every minute for record-keeping and required approximately 0.25 s (including some associated processing). Faster scans at intervals of 2 and 15 s were made of selected measurements for flow and temperature control tasks, respectively. Each manipulated process input had its own digital/analog channel; direct digital control was used in all control loops.

The control computer is a Data General NOVA 4/C with 32 K words of memory. A second computer, the analysis computer, is linked to the control computer through a full duplex asynchronous line. The analysis computer is a NOVA 830 with 64 K words of memory and a 5 million word disk. Both computers were run using a real-time multitasking operating system. All programming was done in FORTRAN except that for supervising the data link, which was written in assembly language. The speed of our machines in floating point matrix operations is about one-tenth that of the IBM PC/XT equipped with a floating point coprocessor.

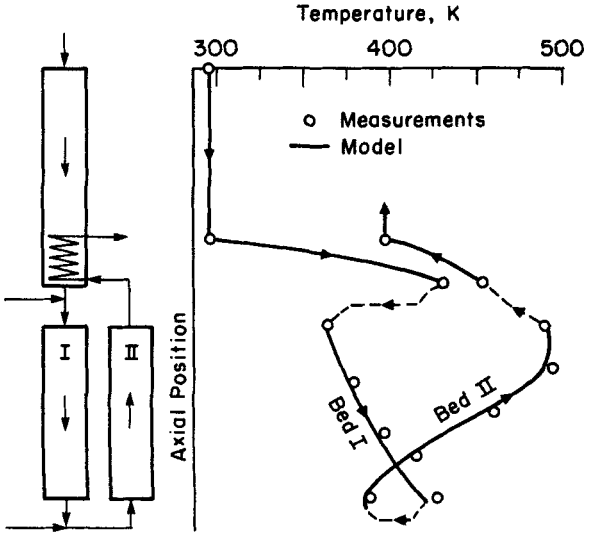

Figure 3. Typical autothermal steady-state temperature profiles.

Steady-State Process Model

The on-line determination of operating conditions performed in the analysis computer requires a steady-state model of the process for predicting the effects of changes in the manipulated inputs. The modeling procedure itself, however, was not an important aspect of this work. The reactor model was previously developed by Silva et al. (1979), and the heat exchanger model follows the same methodology. The model derives from conservation laws of mass and energy simplified by the following major assumptions: no radial gradients, no axial diffusion or conduction, no inter- or intraparticle effects, constant volumetric flows throughout the beds, and constant physical properties. Important features incorporated in the model include a reaction rate dependent on temperature and oxygen concentration to first order, heat loss to the environment through the reactor and exchanger shells, and the distributed nature of the process.

Material and energy balances for each of the reactor beds written in terms of normalized variables take the form:

$$v^i \frac{dy^i}{dz^i} = -R^i \tag{1a}$$

$$v^i \frac{dT^i}{dz^i} = R^i - U_e^i(T^i - T_e) \tag{1b}$$

where

$$R^i = K^i y^i \exp\left(\frac{E_{ref} T^i}{T^i + T_{ref}}\right)$$

and the superscript i refers to reactor bed I or II.

For the heat exchanger the energy balances are:

$$v^{II} \frac{dT^t}{dz^x} = U^x(T^t - T^s) \tag{2a}$$

$$v^x \frac{dT^s}{dz^x} = U^x(T^t - T^s) - U_e^x(T^s - T_e) \tag{2b}$$

where the superscripts t and s refer to tube-side and shell-side quantities, and the superscript x refers to an overall heat exchanger quantity.

Table 2. Typical Operating Conditions

	Feed-Effluent Exchanger		Reactor	
	Shell	Coil	Bed I	Bed II
Length, cm	3.0	15.8	16.5	22.0
Inlet O_2 conc., mol %	1.14	0.01	1.14	0.75
Outlet O_2 conc., mol %	1.14	0.01	0.64	0.01
Conversion, %	0	0	44	99
Inlet temp., K	297	459	420	381
Outlet temp., K	413	406	420	492
Press. at inlet, kPa (psia)	144 (20.8)	113 (16.3)	143 (20.7)	128 (18.5)
Flow rate, std L/s	0.0890	0.1642	0.1204	0.1642
Superficial mass flux, g/cm² · s	0.00177	0.232	0.00242	0.00308
Reynolds no.	9.80	773	1.34†	1.71†
Nominal gas residence time, s	0.154	0.007	0.254	0.265
Thermal wave transit time, s	42*	16**	348‡	365‡
	Bypass flow rate, std L/s	0.0322		
	Quench flow rate, std L/s	0.0334		
	Ambient temp., K	297		

†Based on particle diameter.
*Based on thermal capacitance of both shell and coil
**Based on thermal capacitance of coil only
‡Based on thermal capacitance of catalyst and tube wall.

The variables in these equations are related to the corresponding dimensional quantities (denoted by a ~ overscore) through the following normalizing relations:

$$z^i = \frac{\tilde{z}^i}{\tilde{L}^i_{ref}}; \quad v^i = \frac{\tilde{v}^i}{\tilde{v}_{ref}}; \quad y^i = \frac{\tilde{y}^i}{\tilde{y}^i_{ref}}$$

$$T^i = \frac{\tilde{T}^i - \tilde{T}_{ref}}{\Delta\tilde{T}_{ref}}; \quad \Delta\tilde{T}_{ref} = \frac{(-\Delta\tilde{H}_r)(Mw)\tilde{y}_{ref}}{\rho c_p}$$

$$T_{ref} = \tilde{T}_{ref}/\Delta\tilde{T}_{ref}; \quad E_{ref} = \frac{E/R}{\tilde{T}_{ref}};$$

$$K^i = \frac{k^i P_T Mw \pi R_i^2 L^i}{\rho_f \tilde{v}_{ref}} e^{-E_{ref}}$$

As a matter of convenience, T_e in Eqs. 1b and 2b can be set to zero (corresponding to equivalence with T_{ref}) to further simplify the model. The boundary conditions are obtained from mass and energy balances relating the inputs of each unit to the outputs of the upstream unit and to the feed. In terms of normalized variables, these balances are:

At the bypass mixing point

$$T^{\mathrm{I}}(0) = \frac{v^x}{v^{\mathrm{I}}} e_{x1} T^s(1) + \frac{B}{v^{\mathrm{I}}} T_F \tag{3a}$$

$$y^{\mathrm{I}}(0) = y_F \tag{3b}$$

At the quench mixing point

$$T^{\mathrm{II}}(0) = \frac{v^{\mathrm{I}}}{v^{\mathrm{II}}} e_{12} T^{\mathrm{I}}(1) + \frac{Q}{v^{\mathrm{II}}} e_{12} T_F \tag{3c}$$

$$y^{\mathrm{II}}(0) = \frac{V^{\mathrm{I}}}{v^{\mathrm{II}}} y^{\mathrm{I}}(1) + \frac{Q}{v^{\mathrm{II}}} y_F \tag{3d}$$

At the exchanger coil inlet

$$T^t(1) = e_{2x} T^{\mathrm{II}}(1) \tag{3e}$$

At the exchanger shell inlet

$$T^s(0) = T^x_{in} \tag{3f}$$

where

$$e_{x1} = \frac{2v^x - N_{x1}}{2v^x + N_{x1}},$$

$$e_{12} = \frac{2v^{\mathrm{II}} - N_{12}}{2v^{\mathrm{II}} + N_{12}},$$

$$e_{2x} = \frac{2v^{\mathrm{II}} - N_{2x}}{2v^{\mathrm{II}} + N_{2x}},$$

and N_{x1}, N_{12}, and N_{2x} are respectively the number of heat-transfer units for heat loss at the junction of the exchanger and bed I, bed I and bed II, and bed II and the exchanger.

The sets of differential equations, Eqs. 1 and 2, were transformed to a larger set of algebraic equations using an orthogonal collocation approximation (Villadsen and Michelsen, 1978). The collocated model has the following form:

$$\begin{bmatrix} y^i \\ T^i \end{bmatrix} = G^i \begin{bmatrix} y^i(0) \\ T^i(0) \end{bmatrix}$$

$$\begin{bmatrix} T^t \\ T^s \end{bmatrix} = G^x \begin{bmatrix} T^t(1) \\ T^s(0) \end{bmatrix}$$

where y^i is the vector of fluid concentrations at the collocation locations in reactor bed i, and anlogous definitions apply to T^i,

T^i, and y^s. Also,

$$G^i = \left[\begin{array}{c|c} \dfrac{-C_o^i A_{c,o}^i}{\dfrac{-K^i}{v^i} B_1^i E^i C_o^i A_{c,o}^i} & \dfrac{0}{-B_1^i A_{c,o}^i} \end{array}\right]$$

$$G^x = \left[\begin{array}{c|c} \dfrac{-\left[I + \dfrac{(U^x)^2}{v^x v^{II}} B_2^x I_c M B_1^x I_c\right] B_2^x A_{c,o}^x}{\dfrac{-U^x}{v^x} M B_1^x I_c B_2^x A_{c,o}^x} & \dfrac{\dfrac{-U^x}{v^{II}} B_2^x I_c M B^x A_{c,o}^x}{-M B_1^x A_{c,o}^x} \end{array}\right]$$

$$C_o^i = \left[A_c^i + \frac{K^i}{v^i} E^i\right]^{-1} \qquad E = \operatorname{diag}\left[\exp\left(\frac{E_{ref} T_j^i}{T_j^i + T_{ref}}\right)\right]$$

$$B_1^i = \left[A_c^i + \frac{U_e^i}{v^i} I\right]^{-1} \qquad I_c = \begin{bmatrix} 0 & & 1 \\ & \iddots & \\ 1 & & 0 \end{bmatrix}$$

$$M = \left[I - \frac{(U^x)^2}{v^x v^{II}} B_1^x I_c B_2^x I_c\right]^{-1} \qquad B_1^x = \left[A_c^x + \frac{(U^x + U_e^x)}{v^x} I\right]^{-1}$$

$$B_2^x = \left[A_c^x + \frac{U^x}{v^{II}} I\right]^{-1}$$

A_c^i and A_c^x are collocation matrices for the reactors and heat exchanger; $A_{c,o}^i$ and $A_{c,o}^x$ are collocation vectors. In accordance with earlier studies (Silva et al., 1979), the collocation order for the two reactor beds was chosen as seven. A collocation order of four was found to be sufficient for the heat exchanger.

The reactor curves, examples of which are displayed in Figure 2, were calculated by use of the collocation approximation to Eq. 1 and 3a–d. Equations 2 and 3e–f, similarly approximated, were used for the heat exchanger curves. The coordinated use of these two types of calculations to determine the operating steady state of the reactor-exchanger system is described in a later section.

The model contains 11 physical and eight operational parameters, which are listed in Table 3. In the physical grouping, all but the two preexponential reaction rate parameters were considered constant from day to day, month to month. The heat-transfer coefficients were determined from independent steady-state experiments wherein hot hydrogen gas was passed through the process and temperature drops between relevant points were measured. The heat-transfer parameters express the number of heat-transfer units, and it is seen that those corresponding to heat loss from the various modules and junctions are small but not insignificant. The activation energy parameter was chosen following Silva (1978) to match reactor steady-state gains. The preexponential parameters varied from day to day owing to the slow deactivation of the catalyst. Up-to-the-minute estimates of their values were obtained by fitting model-predicted temperature and concentration profiles to quasi-steady-state profiles obtained from temperature measurements at three or four locations in each bed. A computer program developed by Silva accomplished this within about 3 min upon command; the calculation used the weighted nonlinear least-squares method of Marquardt (1963). It is noticed that the reaction rate constant differs appreciably between beds even though the catalyst and conditions for its activation were the same. Figure 3 shows a typical fit of the model to the measured temperature and concentration profiles. Such fits to the measurements were displayed graphically on the operator's video display upon command.

Table 3. Steady-State Model Parameters

	Normalized Value	Corresponding Dimensional Value
		Physical Parameters
U_e^I	0.216	u_e^I = 0.391 W/m² · K (0.690 Btu/h · ft² · °F)
U_e^{II}	0.082	u_e^{II} = 0.112 W/m² · K (0.198 Btu/h · ft² · °F)
U^x	0.946	u^x = 12.6 W/m² · K (22.2 Btu/h · ft² · °F)
U_e^x	0.018	u_e^x = 0.179 W/m² · K (0.316 Btu/h · ft² · °F)
N_{x1}	0.145	
N_{12}	0.126	
$N2x$	0.172	
K^I	0.0112	k^I = 0.0500 gmol/cm³ · s · kPa
K^{II}	0.0206	k^{II} = 0.0911 gmol/cm³ · s · kPa
E_{ref}	15.2	$\tilde{E}/R$ = 4,500 K
T_{ref}	1.77	$\tilde{T}_{ref}$ = 297 K; $\Delta\tilde{T}_{ref}$ = 167 K
		Operational Parameters
v^I	0.725	$\tilde{v}^I$ = 0.1204 L/s
v^{II}	0.925	$\tilde{v}^{II}$ = 0.1642 L/s
v^x	0.532	$\tilde{v}^x$ = 0.0890 L/s
Q	0.200	$\tilde{Q}$ = 0.0334 L/s
B	0.193	$\tilde{B}$ = 0.0322 L/s
T_F	0.0	$\tilde{T}_F$ = 297 K
T_{in}^x	0.0	T_{in}^x = 297 K
y_F	1.14	$\tilde{y}_F$ = 0.0114 mol frac

Control System Configuration

The task of averting extinction demands that the control system guide the process quickly and smoothly to new steady-state conditions that can sustain the autothermal state and that are operationally acceptable in other respects. Such a task is accomplished here by driving the two temperatures T_{in} and T_A identified in Figure 1 to new values of set points $(T_{in})_{SP}$ and $(T_A)_{SP}$ upon detection of imminent extinction. The two temperature control loops shown there, when augmented by yet another loop needed to accomplish these tasks, are shown in block diagram form in Figure 4.

Development of the rationale for this configuration begins with the observation that it is highly desirable to block as nearly as possible the continual recirculation of temperature disturbances from reactor bed II through the feed-effluent exchanger to reactor bed I. The diagram shows two feedback control loops, a fast loop and a slow loop, both acting to accomplish the blocking through regulation of T_{in} and both acting from a common measurement and set point. The regulation of T_{in} in this team-like set of loops is accomplished by relegating the long-term adjustment of T_{in} to the slow-acting auxiliary heating system, and the short-term adjustment to the rapid-acting bypass stream. These two temperature control loops are shown also in the process diagram of Figure 1. Because the response of T_{in} to bypass flow input is fast, manipulation of the bypass stream can be quite successful at the short-term control of T_{in} provided the blow-off and valve-closure constraints are avoided. In constrast, the auxiliary exchanger has a delayed effect on the inlet temperature because it acts upstream of the feed-effluent exchanger; any temperature changes made there must propagate through the feed-effluent exchanger before reaching the reactor inlet. Owing to the large wall-to-fluid heat-capacitance ratio in the exchanger module, the thermal transit time is long. Further, the

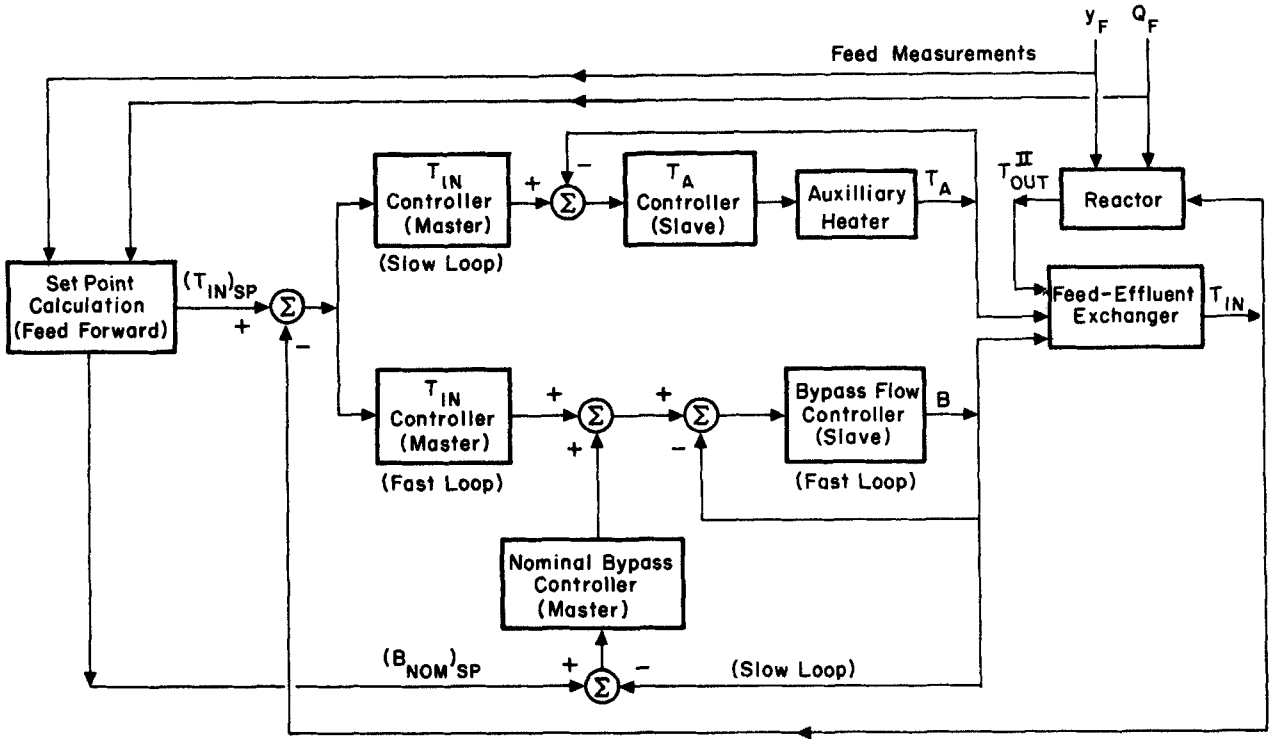

Figure 4. Signal-flow diagram of multiloop control system for guiding reactor to specified steady-state conditions.

auxiliary exchanger system itself has a long time constant. The slowness of the action of the auxiliary exchanger thus makes it unsuitable for fast control action.

The proviso concerning the constraints on the bypass flow rate is critical. Our earlier discussion of steady-state conditions, Figure 2, revealed that significant decreases in feed reactant concentration might not be accommodated by bypass manipulation alone (because of valve closure) and that a certain degree of additional preheating (corresponding to a downward shift of the exchanger curves) would be necessary to establish an autothermal steady state. Such a downward adjustment of the exchanger curve at constant bypass flow is illustrated in Figure 5, showing that a new but different high-temperature steady state can be achieved at the lower feed concentration. The downward shift is accomplished by increasing T_A by an amount corresponding to the change in the exchanger intercept. The new reactor state is characterized by the temperature T_{in}. The value of T_{in} that is deemed best for the new feed concentration is treated in a later section.

One notices from the preceding discussion of the effects of the bypass flow and auxiliary heat exchange that each input acts only on the heat exchanger lines in Figure 2 and 5, leaving the reactor curves unaffected. Bypass flow affects only the slope of the heat exchanger line, influencing the number of heat transfer units achieved, Figure 2. Auxiliary heat exchange affects only the intercept of the heat exchanger line, Figure 5. By suitable combined action of these two inputs, the heat exchanger line can be put into virtually any orientation with respect to the reactor curve, limited only by physical equipment constraints.

The relative amount of each input to be applied to achieve a given result is not unique. There is an overlap in the attainable inlet temperature effected by each input acting alone. The degree of freedom this circumstance provides was exploited by adding a second requirement, namely that the bypass flow rate be brought back to a nominal mid-range value at the new steady state; hence the incorporation of the nominal bypass control loop in the configuration shown in Figure 4. The reasoning behind

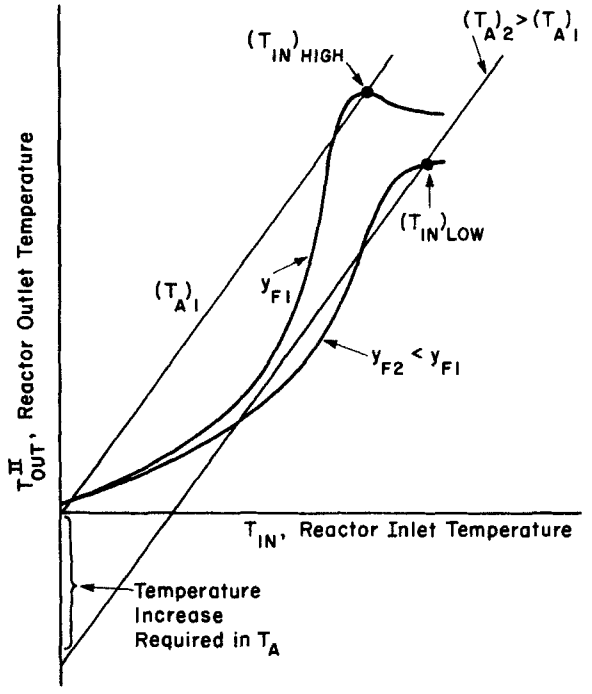

Figure 5. Shift in the reactor system steady state by action of auxiliary heater.

this added requirement relates to the relative speed of response of the two control inputs as discussed above. The auxiliary heat exchange system, being relatively slow, can take over the long-term burden of control and allow the bypass flow, which handles the short-term control task, to return to its nominal value in preparation for any subsequent disturbance. The idea of splitting the control task into dynamic and static components between two inputs was also employed by Wallman et al. (1979) in a linear-quadratic control context. The novelty here is the application of the same idea in a multiloop configuration. The merit of the idea lies in its ability to keep the most effective input, in this case the bypass flow rate, away from constraint limits. Shinskey (1981) describes such a configuration as a generally useful control structure.

The effects of quench flow rate manipulation are much more complex than bypass flow or auxiliary exchanger manipulation. The quench stream flow affects both the feed-effluent exchanger and the reactor in a nonlinear fashion, and dynamically it tends to oppose the effects of the bypass flow control. To avoid such complexity, the quench flow rate was held constant throughout this work. Under such a mode of operation one can interpret the action of the control system as a reorienting of the heat-exchanger line to maintain a desired intersection with the reactor curve, which is unaffected by the control system and determined only by the process.

Thus, when the control system of Figure 4 receives the new set points $(T_{in})_{SP}$ and $(T_A)_{SP}$ that preserve intersection of the exchanger and reactor curves, the inlet temperature T_{in} is driven appropriately to its set point principally by the manipulation of the bypass flow rate. Thermal disturbances from variations in the reactor effluent temperature T^{II} are also attenuated by that controller. Temperature T_A, the auxiliary exchanger output, should be brought to set point as rapidly as possible without overshoot. A special controller employing a time-optimal algorithm sequenced with a Smith predictor was developed for this task (Lappinga and Foss, 1984), but in the work reported here, the startup heater was used with a PI controller in place of the auxiliary exchanger. The bypass controller of Figure 4 is designed to drive the bypass flow slowly to a selected mid-range value. This latter loop may be viewed as a trimming control on the amount of preheating needed to maintain autothermicity while insuring adequate rangeability of the bypass flow rate. It functions like the valve-position controllers described by Shinskey (1979).

With the exception of the special time-optimal controller used in the work of Lappinga and Foss (1984), all of the control loops are digital, single-variable, proportional-integral loops. The standard incremental algorithm was used:

$$u_k = u_{k-1} + K_p \cdot (y_{k-1} - y_k) + K_i \cdot (r_k - y_k) \qquad (6)$$

where u is the manipulated input, y is the controlled variable measurement, r is the set point, and k denotes the sampling instant. Incorporated in each was a provision to guard against reset windup. The flow loops were sampled rapidly, at 2s intervals, while the temperature loops are sampled much more slowly, at 15s intervals. No detailed study was conducted to find optimum sampling rates for each loop. The rates quoted here were selected relative to the characteristic response times of the process and when tested were found to give good results. The control loops were tuned through a combination of root-locus analysis, step testing, and evolutionary adjustments. A typical set of controller settings and performance characteristics is given in Table 4.

Preserving Relative Stability Under Abnormal Conditions

The steady-state conditions of the reactor differ at altered feed concentrations. Indeed, as illustrated in Figure 5, a sustained reduction in feed concentration will likely require an increase in the bed I feed temperature T_{in}. Just what value should be assigned to T_{in} involves considerations beyond those of merely attaining an intersection of the reactor and exchanger operating curves. Maintaining a constant T_{in} in the example of Figure 5 would appear to be undesirable because the new steady state would correspond to an unstable autothermal state (i.e., intersection would occur to the left of the knee). Even though the control system might be capable of stabilizing that state, one would more likely prefer to retain operation at the high-temperature steady state.

The value of T_{in} selected in this work is one that preserves the relative stability of the controlled process under all conditions of operation, normal or abnormal. Such an attribute of any operating process would seem eminently desirable and, indeed, is known to be sought by process operators. Process relative stability may be represented by the location of the eigenvalues or poles (in the complex plane) of a linearized mathematical model of the process. Changes in the feed concentration and flow rate will cause shifts in the poles, but if the steady-state bed inlet temperature T_{in} is appropriately adjusted in coordination with such changes, it is found that the dominant poles remain almost stationary (Metchis, 1982). The shift in T_{in} that accomplishes this was found, through a calculational analysis, to be related to

Table 4. Typical Controller Settings

Loop	Sampling Interval (s)	K_p	K_i	Overshoot (%)	Settling Time s
Q valve	2	1,500% valve/std L/s	1,500% valve/std L/s	0	6
B valve	2	1,500% valve std L/s	1,500% valve/std L/s	0	6
$(B)_{nom}$–B	2	0	0.005	0	2,700
T_{in}–B	15	−167 std L/s/K	−167 std L/s/K	19 (without filter)	360
				0 (with filter)	900
T_{in}–T_A	15	5.4	0.6	0	2,700
T_{in}–Heater	15	32 W/K	8 W/K	0	240

*See Fig. 4.

the location of the peak or knee in the steady-state reactor curves displayed in Figure 5 (i.e., the T_{in} value of the peak). Values of T_{in} displaced a specified number of degrees from the peak were found to hold the location of the dominant poles nearly constant irrespective of the feed concentration or flow rate. The temperature displacement from the peak is termed here the "temperature margin." Thus, the relative stability of the two operating conditions of high and low feed concentration is held constant in the example of Figure 5 because a temperature margin of zero is specified for both [that is, T_{in} is set at the peak at temperatures $(T_{in})_{high}$ and $(T_{in})_{low}$]. Increasing the margin makes the process more stable (poles are shifted deeper into the left half of the complex plane). In some cases, the margin can be taken a few degrees negative before the blow-off constraint is encountered; such operating points are less stable than those with zero or positive margin. In this work, a zero margin was adopted because the dynamic behavior of the reactor-exchanger system seemed nicely positioned between sluggishness and oscillatory motion and because the extent of reaction was nearly evenly distributed between the two beds. Use of the temperature margin as an indicator of process operability is similar to the use of a so-called stability margin by Stephens and Richards (1973), but the use by Metchis (1982) reported here seems to be the first that has made a direct association of such simple measures with the poles of the process. Lewin and Lavie (1984) have recently made a similar investigation in connection with the effect of catalyst activity decline in ammonia synthesis reactors. In current work, a more direct measure of relative stabilty is being sought through the on-line determination of process eigenvalues.

Deciding on the combination of bypass flow rate and auxiliary exchanger temperature capable of achieving a zero temperature margin pertaining to the conditions of the moment requires knowledge of the feed concentration and flow rate. Disturbances in these process variables would likely be known in industrial situations; in our work, they were measured continuously. When changes in these disturbances were observed to exceed a specified threshold, the following sequence was begun to determine values of the bypass flow rate set point and auxiliary exchanger temperature set point and to initiate control action designed to preserve relative stability.

1. A rough estimate of the new $(T_{in})_{SP}$, based on the measured feed concentration and flow disturbance, is imposed on the T_{in} control loop through a first-order filter having a time constant of about 5 min. A gradual imposition of the temperature change is made to minimize the inverse temperature response of this type of reactor (Hoiberg et al., 1971).

2. A calculation is begun immediately to determine an accurate model-based value of $(T_{in})_{SP}$ that preserves stability. This calculation requires about 3 min.

3. Next follows a procedure to select the auxiliary exchanger temperature set point $(T_A)_{SP}$ and the bypass flow set point B_{SP} needed to attain the new $(T_{in})_{SP}$. Any number of procedures may be used. The procedure implemented in our work interrogated the following conditions sequentially and executed the actions stated here for the first one satisfied.

a. Under the presumption that no auxiliary heat input is needed, the bypass flow set point necessary to attain $(T_{in})_{SP}$ is calculated and set provided the flow calculated is not less than 10% of the maximum attainable bypass flow.

b. With the bypass flow assumed to be at 50% of its full range, the auxiliary temperature $(T_A)_{SP}$ and heat input rate necessary to achieve $(T_{in})_{SP}$ is calculated. If the calculated heat input rate is less than the maximum deliverable, B_{SP} is set at 50% and $(T_{in})_{SP}$ is set at the value calculated in step. 2.

c. If condition *b* fails, it is reexamined with the bypass halved. The halving is repeated until an implementable heat rate is found or the calculated bypass flow rate is less than 10% of full range, in which case the operator is informed that a safely operable autothermal steady state cannot be assured and that steps should be taken to shut down the process.

4. Implementation is made of the new set points $(T_{in})_{SP}$ and B_{SP} determined in steps 2 and 3. Set point $(T_A)_{SP}$ is implemented through the cascade from the second temperature controller that acts slowly on the error in T_{in}. Such decisions become available and are executed about 6 min after the disturbance is detected. This analytical and calculational delay is the motivation for the immediate use of rough interim estimates in step 1.

Experimental Testing

Experiments demonstrating extinction

Extinction of reaction in the uncontrolled process is shown in Figure 6. In this experiment, the process was subjected to a 15% decrease in feed concentration at the time marked by the arrow. Temperatures within the first catalyst bed immediately began to fall, owing to the reduced oxygen concentration. When the induced temperature wave reached the second bed, it caused inverse (wrong-way) response of the outlet temperature. The natural feedback of the process allowed the thermal wave to pass repeatedly through the process. The oscillations damped out after only a couple of passes, owing to the heat loss in the laboratory process. Thereafter, it is seen that the extinction proceeded at an accelerating rate. The time scale is important to note: after 4 h the extinction was not yet complete, but was in fact still accelerating. This contrasts with the time required for a thermal wave to pass once through the process, about 15 min. Denn and Lavie (1982) have shown that slow dynamics is a characteristic feature of processes with recycle, being analogous to a positive feedback control loop. It is well known that positive feedback has the effect of increasing process time constants.

The evolution of the reactor temperature profile observed during this slide to extinction is shown in Figure 7. This figure shows the rapid drop of the temperatures in the first bed immediately after the disturbance. This caused the bed II inlet tem-

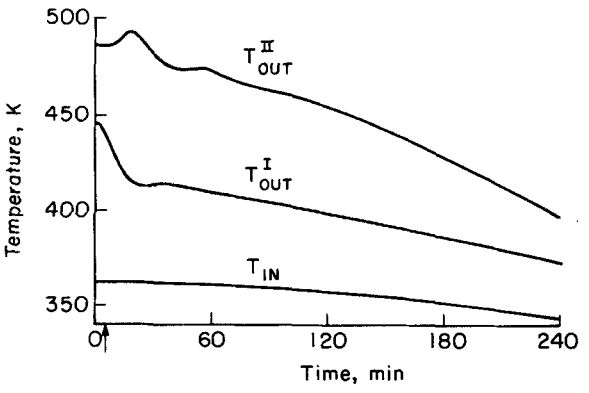

Figure 6. Experimental demonstration of extinction of uncontrolled autothermal reactor.
Feed concentration decrease from 1.15 to 1.00% O_2

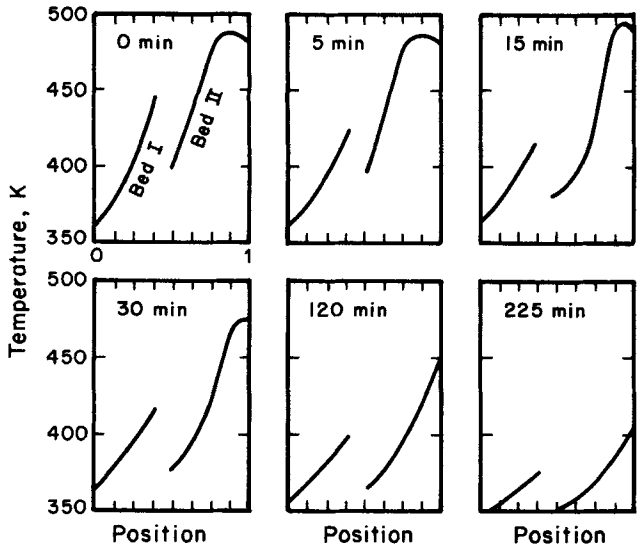

Figure 7. Evolution of reactor temperature profile during extinction of autothermal state.
Extinction caused by 15% decrease in feed oxygen concentration; reactor uncontrolled

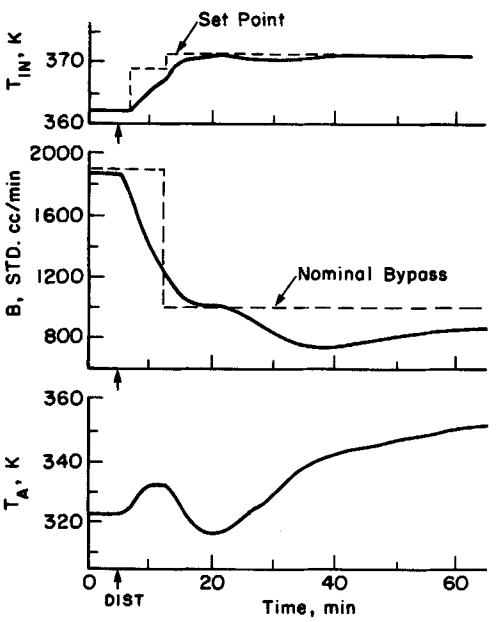

Figure 8. Experimentally observed set points and process input variables responding to commands from extinction analysis program.
Feed concentration decrease from 1.15 to 1.00% O_2

perature to drop as well. However, a buffering effect at the end of the second bed, combined with the wrong-way effect, served to maintain the outlet temperature nearly constant. The buffering effect is due to the reaction being complete, under normal conditions, before the end of the catalyst bed. Any excess of reactant reaching the dead zone is consumed there before it reaches the outlet. This buffering causes the hot spot in the second bed to move in response to changing conditions. In this experiment the hot spot moved down the bed and finally out of the reactor after about 30 min. Once the buffering capacity was exceeded the outlet temperature began to drop rapidly.

The slide to extinction was found to follow a similar but extended trajectory under the single-loop control of T_{in} at constant set point. Such a loop is commonly found in industrial practice. The trajectory was observed to be extended because the control loop did not allow T_{in} to drop as in Figure 6, but when the bypass valve reached a fully closed state, T_{in} and all other reactor temperatures decreased gradually as in Figure 6.

Test of control system to avert extinction

The sequence of events shown in Figures 8 and 9 occurred when our full control system was used to accommodate a feed concentration drop from 1.15 to 1.00% oxygen. A disturbance of this magnitude was considerably larger than the threshold that was set for the implementation of this procedure. An estimated new set point for T_{in} 9°C above its initial value was imposed manually about 1 min after the feed concentration change was detected. Figure 8 shows this change and the resulting rise in both T_{in} and T_A. The rises were purposely slowed by the input filter on the T_{in} set point. The bypass flow rate decreased to effect the increase in T_{in}. After about 6 min the reactor analysis computations provided a more accurate set point value for T_{in}, about 2.5°C higher than the rough estimate. A new nominal bypass flow rate also came with these calculations by the procedure just described. Both new set points were implemented immediately and the control system was allowed to run its course to the new steady conditions as recorded in Figure 8.

The history of the reactor bed temperatures under this control action is shown in Figure 9. The initial rapid drop in bed I temperature and the wrong-way excursions and subseqeunt rapid drop in bed II temperature result from the decreased reaction rate and are similar to those of Figure 6. These initial excursions represent the "free reactor" response: arresting the fall at a particular point in the bed can be achieved with these manipulatable inputs only at the time the corrective thermal wave [which was introduced by a change in $(T_{in})_{SP}$] reaches that point. The wave transit time for each bed is approximately 6 min. Thus, the

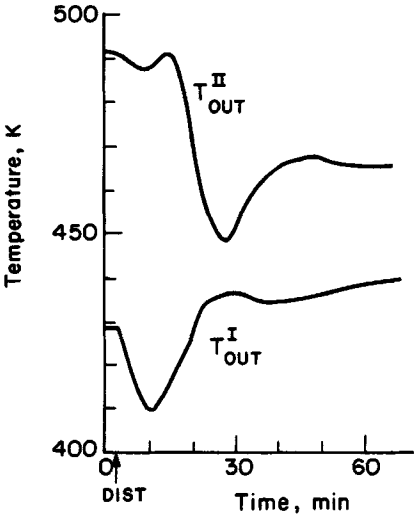

Figure 9. Effluent temperatures of reactor beds in response to a feed concentration decrease from 1.15 to 1.00% O_2 and control actions of Figure 8.

turnaround in bed I temperature is seen to be accomplished in nearly this time; 15 min later the bed II temperature drop is arrested. The temperatures to which the two beds eventually rise are those calculated to yield a temperature margin of zero. These final new stable operating conditions are seen to be reached in about 1 h under the control actions displayed in Figure 9, a time short compared to the 4 or 5 h gradual slide to extinction. The final operating point actually reached was usually slightly different from that predicted by our on-line steady-state analysis because of uncertainties and small changes in system parameters such as system pressure and exchanger heat-transfer coefficients. These variations were of no consequence in achieving an operable state in our experiments, but if need be, simple refinements to model such effects can be made easily in the on-line analysis program.

Experiments in which the full 6 min delay was taken before implementing the new $(T_{in})_{SP}$ revealed that the reactor response was essentially no different from that shown in Figure 9 over the 1 h transient. The bypass flow rate and auxiliary heater temperature, however, were required to make larger excursions to accomplish their tasks. In circumstances where the manipulatable inputs have a narrow rangeability, such demands could saturate the inputs and lead to loss of control.

The evolution of the reactor temperature profile under the action of these procedures to avert extinction is shown in Figure 10. The conditions of operation are similar to those of Figures 8 and 9, but the implementation of control action is delayed for the full 6 min calculational delay. The hot spot in bed II is seen to have moved temporarily to the end of the bed before the inlet temperature was raised; the corrective temperature wave then brought it back to its original position. Such a stabilization of the reactor profiles has resulted from the control system's action to insure continuity of operation and to preserve the relative stability of the controlled process under the new conditions.

Two other types of process upsets were impressed on the reactor system to test the breadth of applicability of the extinction-avoidance system. Step changes in feed flow rate were accommodated without any alteration of the analysis and control procedures, and the control system was observed to conduct the reactor system to safe steady operating points. Reactor temperature responses under flow upsets differ considerably from those of concentration upsets, however (Metchis, 1982). To observe system performance when the reactor's initial state was not steady, closely spaced changes in feed concentration were made in succession. When corrective action in response to the first upset was near midcourse, the second feed change was made. The system performed analyses and made corrections for both upsets with no difficulty.

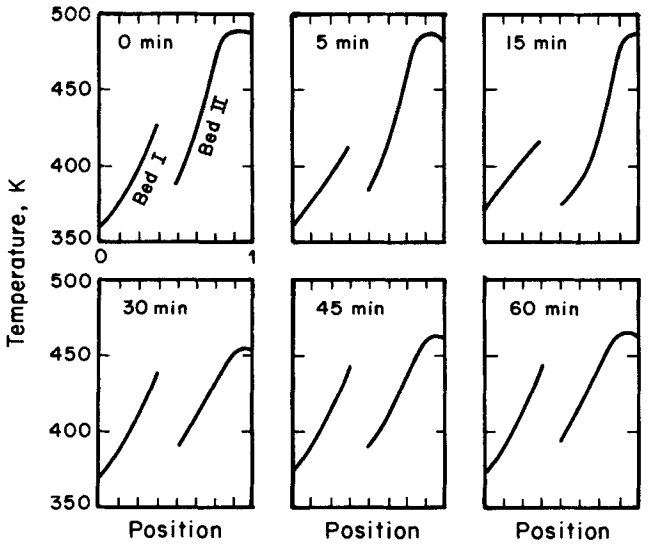

Figure 10. Evolution of reactor temperature profiles under control action that preserves relative stability of autothermal state.
Feed concentration decrease from 1.15 to 1.00% O_2.

Concluding Remarks

One of the major contributions of this work is the development of a modular, real-time procedure for maintaining reactor operability in the face of disturbances that would extinguish the autothermal state. That the procedure is modular is thought to be a feature of considerable practical value. The modules are assuredly familiar to experienced process engineers, namely least-squares parameter determination, a well-known steady-state analysis of autothermal operation, and easily configured systems of conventional single-input/single-output controllers. The modularity contributes to ease of understanding and ease of implementation.

The criteria for selecting the reactor operating conditions rest on the premise that reactors should operate at the same degree of relative stability under all conditions, normal and abnormal. Such a condition is seldom imposed in the direct way it has been here. Here it determines the temperature set point of the feed to the first catalyst bed. That set point has been found to be closely related to the location of the dominant eigenvalues of the reactor-exchanger system and is easily calculated from the reactor and heat exchanger models. The temperature margin parameter used in that determination is a physically interpretable quantity. In work currently under way, we are attempting to make a more direct assessment of relative stability through estimation of system eigenvalues.

That the system functions reliably on a piece of physical equipment is also considered a significant bit of information. The system operates reliably despite structural defects in modeling and numerical errors in the scores of process parameters used in the process model. The system operates without failure even with drifts in calibrations and abrupt jumps in catalyst activity. Prediction accuracy deteriorates in such instances, of course, but with the ability to reevaluate parameters upon command, we have found the system well suited to operating under such instances of duress.

Acknowledgment

This work was supported in part by the National Science Foundation. The authors thank Peter Goodeve and Chris Carvalho for developing the intercomputer communication program and graphical display routines.

Notation

Process parameters and variables given are normalized by their nominal values. Relation to corresponding dimensional quantities is given in text.

A_c, A_{co} = collocation matrix and vector
B = bypass flow rate
E_{ref} = activation energy parameter
K = reaction rate constant

N_{x1}, N_{12}, N_{2x} = number of transfer units for heat loss at joint between heat exchanger and bed I, bed I and bed II, bed II and heat exchanger.
Q = quench flow rate
R = reaction rate Eq. 1b
T = fluid temperature
T_{ref} = reference temperature
U_e = overall heat-transfer coefficient for heat loss to environment
U^x = overall heat-transfer coefficient between shell and tube side of heat exchanger
v = flow rate
y = concentration of oxygen
z = axial position

Superscripts

i = reactor bed designation, I or II
s = heat exchanger shell-side designation
t = heat exchanger tube-side designation
x = general heat exchanger designation

Subscripts

e = ambient designation
F = feed designation

Literature cited

Baddour, R. F., P. L. T. Brian, B. A. Logeais, and J. P. Emery, "Steady-State Simulation of an Ammonia Synthesis Converter," *Chem. Eng. Sci.*, **20**, 281 (1965).

Bonvin, D., R. G. Rinker, and D. A. Mellichamp, "On Controlling an Autothermal Reactor at an Unstable Steady State. I, II, III," *Chem. Eng. Sci.*, **38**, 233, 245, 607 (1983).

Denn, M. M., and R. Lavie, "Dynamics of Plants with Recycle," *Chem. Eng. J.*, **24**, 55 (1982).

Gerdes, K. F., B. E. Stangeland, G. T. S. Chen, and R. J. Gumerman, oral presentation, Joint Auto. Control Conf., San Francisco (1977).

Hoiberg, J. A., B. C. Lyche, and A. S. Foss, "Experimental Evaluation of Dynamic Models for a Fixed-Bed Catalytic Reactor," *AIChE J.*, **17**, 1434 (1971).

Lappinga, A. J., and A. S. Foss, "Rapid Set Point Attainment of Reactor Feed Preheat System and Coordination with Reactor Control," *Proc. Am. Control Conf.*, San Diego, 1624 (1984).

Lewin, D. R., and R. Lavie, "Optimal Operation of a Tube-Cooled Ammonia Converter in the Face of Catalyst Bed Deactivation," *Inst. Chem. Eng. (London) Symp. Ser.*, **87**, Pergamon, 393 (1984).

Luss, D., and N. R. Amundson, "Stability of Loop Reactors," *AIChE J.*, **13**, 279 (1967).

McDermott, P. E., and D. A. Mellichamp, "Pole Placement Self-Tuning Control of Unstable, Nonminimum-Phase Systems," *Proc. Am. Control Conf.*, San Francisco, 825 (1983).

McDermott, P. E., D. A. Mellichamp, and R. G. Rinker, "Multivariable Self-Tuning Control of a Tubular Autothermal Reactor," *Proc. Am. Control Conf.*, San Diego (1984).

Marquardt, D. W., *J. Soc. Ind. Appl. Math.*, **11**, 431 (1963).

Metchis, S. G., Ph. D. Thesis, "Averting Extinction in Operating Autothermal Catalytic Reactors," Univ. California, Berkeley (1982).

Orcutt, J. C., and D. E. Lamb, "Stability of a Fixed-Bed Catalytic Reactor System with Feed-Effluent Heat Exchange," *Proc. 1st World Cong. IFAC*, Basel, **4**, 274 (1960).

Shinskey, F. G., *Process Control Systems*, McGraw-Hill, New York, 150, (1979).

———, *Controlling Multivariable Processes*, Instrument Soc. of America, Chapel Hill, NC, ch. 10 (1981).

Silva, J. M., Ph. D. Thesis, "Multi-bed Catalytic Reactor Control Systems: Configuration Development and Experimental Testing," Univ. California, Berkeley (1978).

Silva, J. M., P. H. Wallman, and A. S. Foss, "Multibed Catalytic Reactor Control Systems: Configuration Development and Experimental Testing," *Ind. Eng. Chem.*, **18**(4), 383 (1979).

Stephens, A. D., and R. J. Richards, "Steady State and Dynamic Analysis of an Ammonia Synthesis Plant," *Automatica*, **9**, 65 (1973).

van Heerden, C., "Autothermic Processes: Properties and Reactor Design," *Ind. Eng. Chem.*, **45**, 1242 (1953).

———, "The Character of the Stationary State of Exothermic Processes," *Chem. Eng. Sci.*, **8**, 133 (1958).

Villadsen, J., and M. L. Michelsen, *Solution of Differential Equation Models by Polynomial Approximation*, Prentice-Hall, Englewood Cliffs, NJ (1978).

Wallman, P. H., J. M. Silva, and A. S. Foss, "Multivariable Integral Controls for Fixed-Bed Reactors," *Ind. Eng. Chem.*, **18**(4), 392 (1979).

Wong, C., D. Bonvin, and D. A. Mellichamp, "On Controlling an Autothermal Reactor at an Unstable Steady State. IV," *Chem. Eng., Sci*, **38**, 619 (1983).

Manuscript received Aug. 22, 1986, and revision received Feb. 4, 1987.